JOURNAL OF IMAGING SCIENCE AND TECHNOLOGY • Volume 43, Number 5, September/October 1999

Mechanistic Aspects of Hole and Electron Injection into Organic Transport Materials

J. Rommens, M. Van der Auweraer* and F. C. De Schryver

Laboratory for Molecular Dynamics and Spectroscopy, KU Leuven, Department of Chemistry, Heverlee, Belgium

The field, temperature and concentration dependence of the dark injection of holes and electrons from metal electrodes into molecular dispersions of respectively 5'-[4-[bis(4-ethylphenyl)amino]phenyl]-N,N,N',N'-tetrakis(4-ethylphenyl)-[1,1':3',1''-terphenyl]-4,4''-diamine and 1,3-bisdicyanomethylene-2-methyl-allyl-indane in polymers has been investigated. All results point to a two step process: in a first step charge carriers are injected to the bottom of the potential well created by an image potential between the charge transport material and the electrode. The competition between escape of the charge carriers from this well and recombination with empty levels in the electrode governs the final rate of charge carrier injection. While in a qualitative way this approach resembles an extension to doped polymers of the Willig-Gerischer model, developed for organic single crystals, a quantitative description of this system requires us to consider also the diagonal and non-diagonal disorder of the hole transport material.

Journal of Imaging Science and Technology 43: 450–459 (1999)

Introduction

While the dark and photosensitized injection of charge carriers in inorganic semiconductors[1] or organic single crystals has been studied extensively,[2] much less is known about injection into amorphous organic materials.[3–5] However, knowledge and control of the injection of charge carriers into charge transport media are essential for the understanding of xerographic[6] and electroluminescent[7] materials. A major difference between the transport in organic amorphous media and in single crystals is the occurrence of diagonal and non-diagonal disorder. Bässler and coworkers developed a transport model, which describes the transport as a hopping process in a Gaussian Density of States (DOS).[8] This disorder is also expected to influence the injection.[9–12]

The charge transport properties of molecular dispersions of the hole transport molecule 5'-[4-[bis(4-ethylphenyl)amino]phenyl]-N,N,N',N'-tetrakis (4-ethylphenyl)-[1,1':3',1''-terphenyl]-4,4''-diamine (p-EFTP)[13–15] and of the electron transport molecule 1,3-bisdicyanomethylene-2-methyl-allyl-indane(ADCMI)[16] have been studied extensively earlier. In order to know more about the hole injection process in polymers, molecularly doped with p-EFTP or ADCMI, the polymers were contacted with metal electrodes characterized by a range of work functions. These results confirm earlier reports where electrolytic contacts were used for the dark[17] and photosensitized[18] injection of holes in polycarbonate films loaded with p-EFTP. The aim of the present contribution is to examine the generality of result obtained earlier for p-EFTP by the influence of the concentration and the chemical structure (electron versus hole transport) of the transport molecules. For all systems the experimental results can be discussed in a qualitative way in the framework of the Willig-Gerischer model,[2] quantitative agreement would however require the explicit consideration of diagonal and non-diagonal disorder.[9–12]

Experimental

The molecular structures of 5'-[4-[bis(4-ethylphenyl)amino]phenyl]-N,N,N',N'-tetrakis(4-ethylphenyl)-[1,1':3',1''-terphenyl]-4,4''-diamine (p-EFTP),1,3-bisdicyanomethylene-2-methyl-allyl-indane (ADCMI) and the polycarbonate are displayed in Scheme 1.

The preparation and purification of p-EFTP and ADCMI have been described elsewhere.[19,20] The polycarbonate was obtained from Mobay Chemicals (Makrolon 5700) and used without further purification. Polystyrene was obtained from Bayer and used without further purification. Samples shown in Fig. 1, were prepared by dissolving the appropriate ratios of p-EFTP or ADCMI and the polycarbonate or polystyrene in dichloromethane, followed by coating the resulting solution on polyethylene terephthalate substrates that had previously been coated with a thin layer of Al. The concentrations are given in % weight. To reduce the residual solvent concentration, the samples were heated to 50°C for 16 h. Afterwards the counter electrode was evaporated in high vacuum (Al, Au) or pressed to the sample (Ga). The thickness of the polymer films (between 10 and 20 μm) was determined using a Lichtschnittmicroscope (Zeiss). The error on the thickness amounts from

---

Original manuscript received December 7, 1998

* To whom correspondence should be addressed

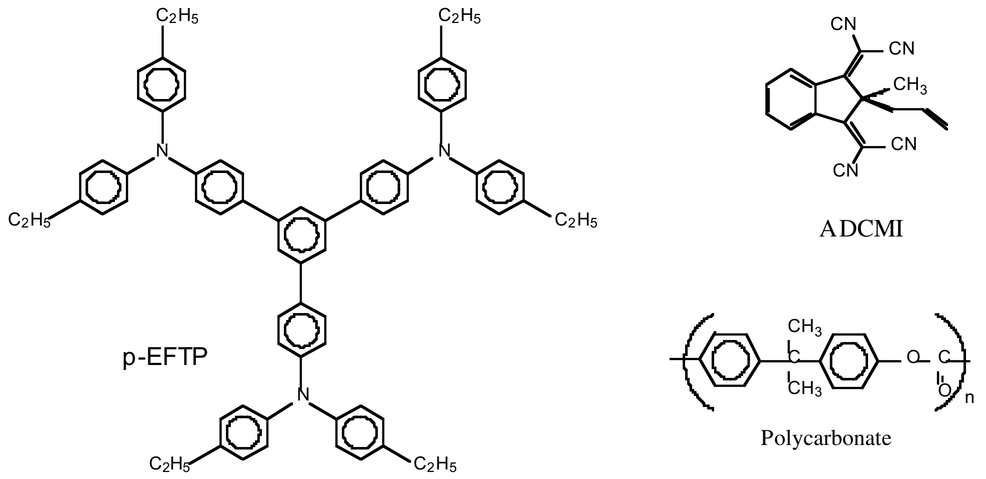

Scheme 1. Molecular structure of p-EFTP: 5'- [4-[bis (4-ethylfenyl) amino] fenyl] - N,N,N',N', -tetrakis (4-ethylfenyl) - [1,1':3',1"-terfenyl] - 4,4"-diamine; 1,3-bisdicyanomethylene-2-methyl-allyl-indane (ADCMI) and PC: bisphenol-A-polycarbonate.

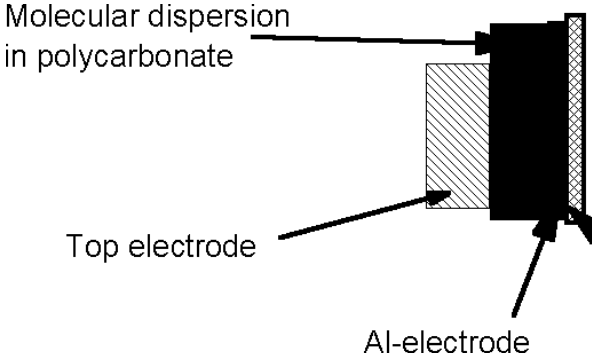

Figure 1. Structure of the samples

1 to 2 µm, which results in an error of 10 to 20% on the calculated field strengths.

To investigate the currents a triangular wave generator was used to create a voltage between 0 and 5 V, which was amplified by a factor 200 using a "Kepco OPS 2000" amplifier. The current was detected with a "Keithley 610 C" electrometer. To protect the Keithley in case of a short circuit or a break down of the sample, a protective device was used, based on a MOSFET where the source was removed or a pair of diodes INTEL 3459, mounted in the blocking directions. The experiments were performed under the conditions where the low voltage resistance of the diode was much larger than the input resistance of the Keithley (10^6 to 10^{10} Ω). The input resistance of the Keithley was at least 20 times smaller than the resistance of the sample to make sure that the diode or the MOSFET were always in blocking (high impedance) regime and to assure that the voltage drop over the electrometer is always negligible to that over the sample.

Results and Discussion

Field Dependence of the Hole Current Density Injected Into Molecular Dispersions of P-EFTP. The concentration dependence of the hole current density injected in p-EFTP confirms earlier suggestions that this process must be described in the framework of the Willig-Gerischer model rather than the Fowler-Nordheim or Richardson-Schottky model. According to the Willig-Gerischer model[2,21] developed for charge carrier injection into single crystals, the injection can be considered as a two step process. In the first step an electron is injected into a molecule close to the interface with a rate v_{inj} ($\mathrm{cm}^{-2}\,\mathrm{s}^{-1}$). It is bound to the interface by an image potential[22–24] (Fig. 2). The escape with a rate constant k_{esc} ($\mathrm{cm\ s}^{-1}$) from the one dimensional potential well into the crystal bulk competes with recombination with rate constant k_{rec} ($\mathrm{cm\ s}^{-1}$) with empty levels above the Fermi-level of the electrode (Fig. 3). In this framework the current density is given by:

$$j = ev_{inj}\,\frac{k_{esc}}{k_{esc}+k_{rec}} \qquad (1)$$

with

$$k_{esc} = \frac{D\exp\left[\dfrac{-eU(R_0)}{kT}\right]}{\int_{R_0}^{\infty}\exp\left[\dfrac{-eU(R)}{kT}\right]dR} \qquad (2)$$

with

$$U(R) = -\,\frac{e}{16\,\pi\,\varepsilon_r\,\varepsilon_0\,R} - ER \qquad (3)$$

where D is the diffusion coefficient of the charge carriers ($\mathrm{cm}^2\,\mathrm{s}^{-1}$) and R_0 (cm) the distance from the interface where the electron arrives after the primary injection step and e the elementary charge (1.6×10^{-19} C). ε_r is the dielectric constant of the sample for which a value of 3 is used. ε_0 ($8.85 \times 10^{-14}\ \mathrm{CV}^{-1}\mathrm{cm}^{-1}$) is the permittivity of vacuum. $U(R)$ and R correspond to the electrostatic potential (V) and the distance to the electrode (cm), while E corresponds to the applied field ($\mathrm{V\ cm}^{-1}$). The diffusion coefficient is related to the mobility µ ($\mathrm{cm}^2\mathrm{V}^{-1}\,\mathrm{s}^{-1}$) by the Stokes-Einstein relation.

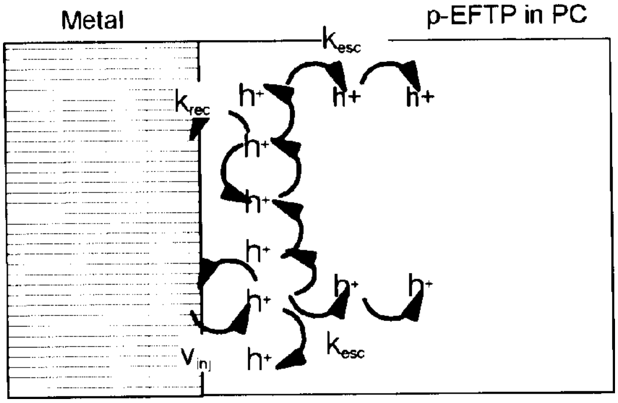

Figure 2. Model for hole injection at an interface between a metal electrode and a molecular dispersion of p-EFTP in polycarbonate.

$$D = \frac{\mu}{ekT} \tag{4}$$

where k is the Boltzmann constant ($1.38 \times 10^{-23}\ J\ K^{-1}$) and T the temperature (K). While for the single crystals[25] of anthracene and perylene the hole mobility is field independent up to 5×10^5 V cm^{-1}, this is not the case for molecular dispersions of p-EFTP[13–15] or ADCMI.[16] However, taking into account that in the image potential well the electric field is opposite to the applied field and that at the top of the image potential barrier the field becomes zero, the mobility extrapolated to zero field was used in Eq. 4. When k_{esc} can be neglected compared to k_{rec} the current density is given by:

$$j = \frac{ev_{inj}k_{esc}}{k_{rec}} \tag{5}$$

As in this model the field dependence of v_{inj} is only marginally[2,21] the field dependence of the hole current density should reflect that of k_{esc}. The latter only depends on the value of the parameter R_0. Therefore in Fig. 4 the field dependence of the current density, normalized at 2.0×10^5 V cm^{-1} is plotted together with values of k_{esc} normalized at 2.0×10^5 V cm^{-1} for three different values of R_0. Note that for the situation where a negative voltage was applied to a gold or silver-magnesium (1/10) top-electrode the current is actually due to the hole injection by the aluminum back electrode.[17] While the field dependence of the hole current density varies only marginally between the different electrodes or between polycarbonate and polystyrene, it is always steeper than the field dependence of k_{esc}. Even for a physically unrealistic "starting position" 2 Å from the interface the variation of k_{esc} is still shallower than that of the current density. This direction of the discrepancy also suggests that the field dependence of the current density cannot be described as a combination of an infinite sink ($k_{rec} \rightarrow \infty$) and a large (10 or 20 Å) thermalization distance of the injected holes.[22,24]

This could be due to the fact that, contrary to the earlier assumption also v_{inj} is field dependent. v_{inj} describes actually an electron transfer process. Changing the applied field changes the free energy of this electron transfer process. When k_{esc} is much smaller than k_{rec} the current density is given by

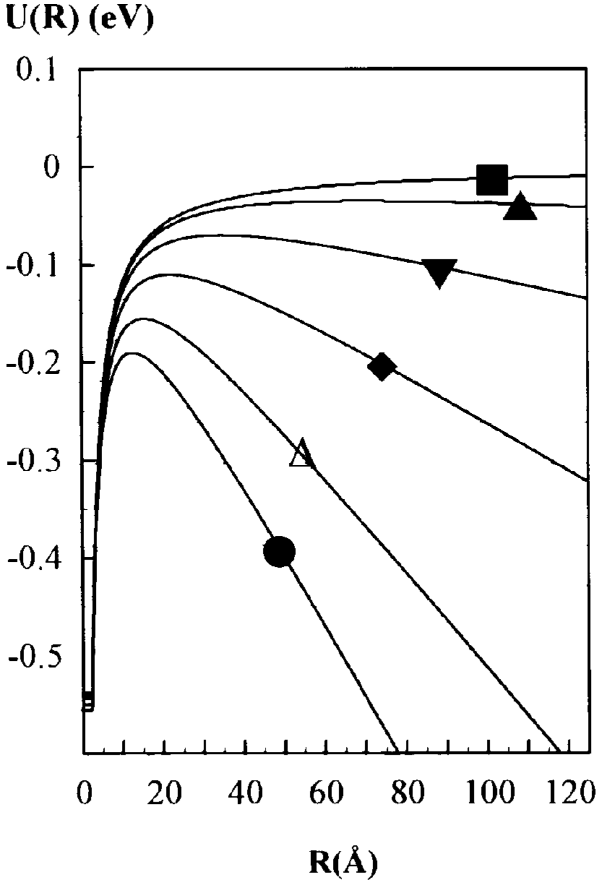

Figure 3. Electrostatic potential in an organic material with $\varepsilon_r = 3$ in contact with a metal electrode. In the absence of an applied potential $U(\infty) = 0$. R_0 equals 4 Å. ■: 0 V cm^{-1}, ▲: 2.5×10^4 V cm^{-1}, ▼: 1.0×10^5 V cm^{-1}, ◆: 2.5×10^5 V cm^{-1}, Δ: 5.0×10^5 V cm^{-1}, ●: 1.0×10^6 V cm^{-1}.

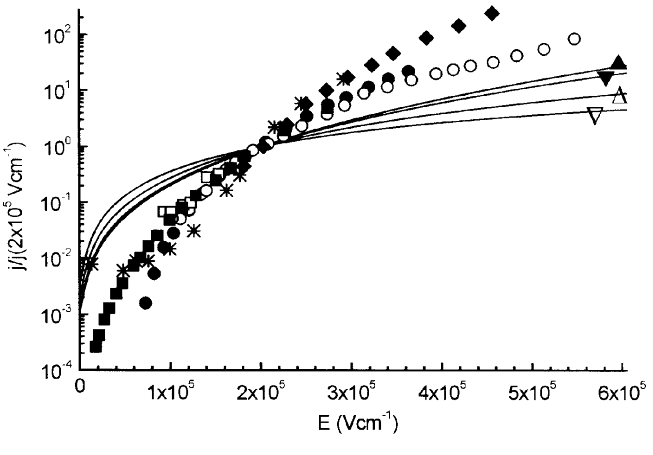

Figure 4. Field dependence of the injected hole current density and the rate constant of escape of the holes in the bulk for a dispersion of 50% p-EFTP in polycarbonate (thickness 11 μ) and polystyrene (thickness 9 μ); the current densities and rate constants are normalized at 2.0×10^5 V cm^{-1}; ◆: positive Al-top electrode, ■: positive gold top electrode, ●: positive Ag-Mg top electrode, ❑: negative Au top electrode, **O**: negative Ag-Mg top electrode, *: negative Au top electrode, injection in polystyrene, ▲: R_0 = 2 Å, ▼: R_0 = 4 Å, Δ: R_0 = 10 Å, ∇: R_0 = 20 Å.

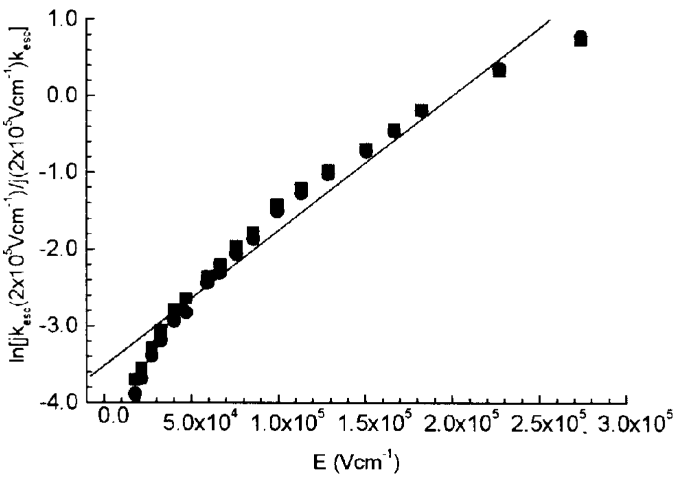

Figure 5. Field dependence of j/k_{esc}, for hole injection from an Au top electrode into 50% p-EFTP in polycarbonate. The thickness of the sample sample amounts to 11 μ. The data are normalized at 2.0×10^5 V cm^{-1}, ●: for R_0 = 4 Å, ■: for R_0 = 2 Å, the slope of a linear regression amounts to $1.8 \pm 0.1 \times 10^{-5}$ cmV^{-1}, correlation coefficient equals 0.979.

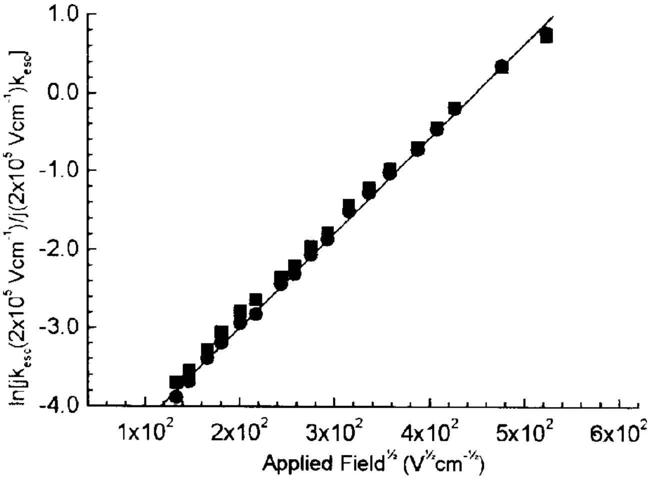

Figure 6. Dependence of j/k_{esc}, for hole injection from an Au top electrode into 50% p-EFTP in polycarbonate on the square root of the applied field. The thickness of the sample amounts to 11 μ. The data are normalized at 2.0×10^5 V cm^{-1}, ●: for R_0 = 4 Å, ■: for R_0 = 2 Å, the slope of a linear regression amounts to $1.21 \pm 0.01 \times 10^{-2}$ cm-V^{-}, correlation coefficient equals 0.9992.

$$j = \frac{k_{esc} v_{inj}}{k_{rec}} = k_{esc} \exp^{\frac{-\Delta G^0_{inj}}{kT}} \approx k_{esc} \exp^{\frac{-\Delta H^0_{inj}}{kT}} \tag{6}$$

where ΔG^o_{inj} and ΔH^o_{inj} correspond to the standard free enthalpy and standard enthalpy change associated with the primary injection. ΔG^o_{inj} is given by

$$\Delta G^o_{inj}(E) = \Delta G^o_{inj}(0) - eFR_0 \tag{7}$$

where $\Delta G^o_{inj}(0)$ is the free enthalpy change when no external field is applied. Hence plotting

$$\ln\left(\frac{j\, k_{esc}\left(2 \times 10^5 Vcm^{-1}\right)}{j\left(2 \times 10^5 Vcm^{-1}\right) k_{esc}}\right)$$

versus the applied field should yield a straight line with a slope eR_0/kT. When

$$\ln\left(\frac{j\, k_{esc}\left(2 \times 10^5 Vcm^{-1}\right)}{j\left(2 \times 10^5 Vcm^{-1}\right) k_{esc}}\right)$$

is plotted versus the applied field using values of k_{esc} calculated with R_0 equal to 2 Å or R_0 equal to 4 Å, the slope of a linear regression of the data corresponds to a value of 46 ± 3 Å for R_0. Such large thermalization distance is not only unrealistic for thermally injected holes; it furthermore leads to a highly inconsistent model as the values of R_0 used to calculate the field dependence of k_{esc} and that obtained from the slope of the plot in Fig. 5 differ by an order of magnitude! Furthermore the fit of the data points to the least square line is far from good as shown in Fig. 5. Here one should note that when for the same sample

$$\ln\left(\frac{j\, k_{esc}\left(2 \times 10^5 Vcm^{-1}\right)}{j\left(2 \times 10^5 Vcm^{-1}\right) k_{esc}}\right)$$

is plotted versus the square root of the applied field, a perfect fit with a slope of $1.21 \pm 0.01 \times 10^{-2}$ cm^{½}V$^{-½}$ is obtained (Fig. 6). This fit can however not be rationalized in any current model. Hence one can conclude that the difference between the field dependence of the hole current density and that of k_{esc} is too large to be due to the field dependence of v_{inj}. A more plausible explanation is that, as argued by Arkhipov and co-workers,[9] the discrepancy is due to the superposition of a random distribution of energy levels of the injected holes in the image potential barrier.

Concentration Dependence of the Hole Current Density Injected into Molecular Dispersions of p-EFTP. The hole current injected by an aluminum electrode in p-EFTP increases upon increasing the concentration of the charge transport molecule. As the hole current density increases much faster than linear with the concentration of the transport molecule, it was attempted to rationalize it in the framework of the model given in Fig. 2. In this model k_{rec} does not depend upon the concentration of the charge transport molecules. k_{esc} depends upon the concentration of the transport molecule through D or μ. v_{inj} can be expected to be proportional to the density of states at the valence band edge, which can, due to the small bandwidth be put equal to the concentration of the transport molecule (cm^{-3}).

$$v_{inj} = k_{ox} N_{VB} \tag{8}$$

where k_{ox} (cm s^{-1}) is the rate constant for the interfacial charge transfer between the electrode and the polymer film. Hence under conditions where k_{esc} can be neglected compared to k_{rec} the current density will be given by:

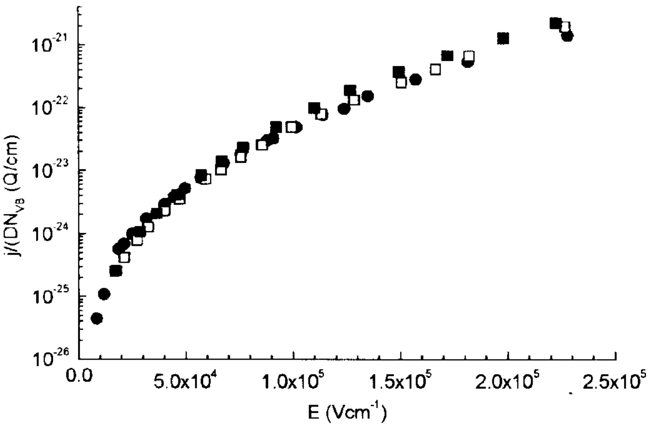

Figure 7. Influence of the applied field on j/DN_{VB} for a molecular dispersion of p-EFTP in polycarbonate; ●: 40% (thickness 11 μ), □ : 50% (thickness 11 μ), ■: 60% (thickness 9 μ).

$$j = \frac{eDk_{ox}N_{VB}}{k_{rec}} \frac{\exp\left[\frac{-U(R_0)}{kT}\right]}{\displaystyle\int_{R_0}^{\infty} \exp\left[\frac{-U(R)}{kT}\right] dR} \tag{9}$$

According to Eq. 9, j/DN_{VB} should be independent the concentration of the transport molecules as shown by the coincidence of the curves in Fig. 7 for p-EFTP in polycarbonate. As upon increasing the p-EFTP concentration from 40% to 60% N_{VB} changes only marginally, this means that the current density is proportional to the charge carrier mobility. Such a dependence is impossible to explain in the framework of a Fowler-Nordheim[26–28] or Richardson Schottky[25–27] model.

Temperature Dependence of the Hole Current Density Injected into Molecular Dispersions of p-EFTP. The logarithm of the current density injected into a 50% dispersion of p-EFTP in polycarbonate varies between 293 K and 337 K linearly versus the inverse temperature. The slope of this linear relationship becomes shallower (Fig. 8) upon increasing the applied field from 9.1 × 10^3 V cm^{-1} to 1.8 × 10^5 V cm^{-1}. This corresponds to a decrease of the activation energy from 0.75 eV at 9.1 × 10^3 V cm^{-1} to 0.47 eV at 1.8 × 10^5 V cm^{-1}. According to Eq. 10 the image potential barrier ΔU(eV) should decrease proportional to $E^{1/2}$ when the term eER_0 can be neglected. The latter simplification can be made as R_0 (4 to 5 Å) is always much smaller than the width of the barrier.

$$\Delta U = -\sqrt{\frac{e}{4\,\pi\,\varepsilon_r\,\varepsilon_0}}\sqrt{E} + \frac{e}{16\pi\varepsilon_r\varepsilon_0 R_0} + ER_0 \tag{10}$$

When the activation energy E_a (eV) is plotted versus $E^{1/2}$ (Fig. 9) a linear relationship is observed. The slope amounts to 9.2×10^{-4} $\mathrm{cm}^{1/2}\mathrm{V}^{-1/2}$ while according to Eq. 10 it should be no more than 2.19×10^{-4} $\mathrm{V-cm}^{1/2}$. This phenomenon was also observed at the RhSi/Si interface where it was attributed to "static lowering".[29]

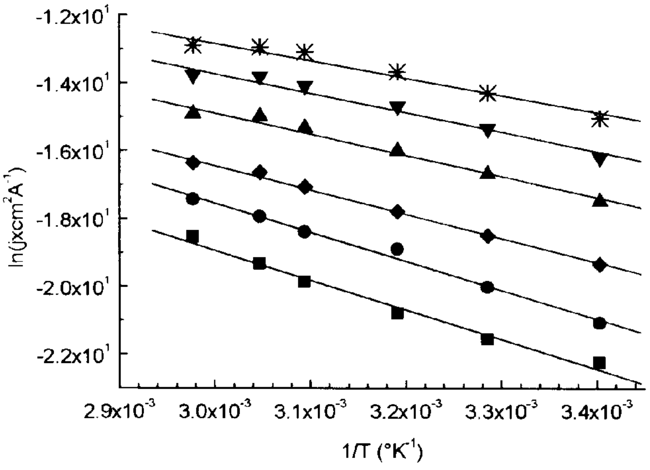

Figure 8. Arrhenius plot of the sensitized hole current injected by an Au top electrode in a 50% dispersion of p-EFTP in polycarbonate (thickness 11 μ); ■: 9.0 × 10^3 V cm^{-1}, ●: 1.82 × 10^4 V cm^{-1}, ◆: 4.55 × 10^4 V cm^{-1}, ▲: 9.01 × 10^4 V cm^{-1}, ▼: 1.36 × 10^5 V cm^{-1}, *: 1.82 × 10^5 V cm^{-1}.

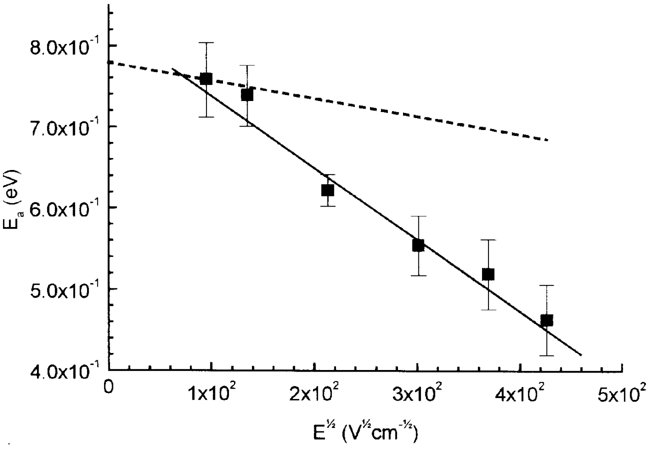

Figure 9. Plot of the activation energy for hole injection into a 50% p-EFTP dispersion in polycarbonate (thickness 11 μ) by an Au top electrode, full line: least square plot ρ = 0.979, dashed line plot according to Eqs. 10 and 11.

When the activation energy is extrapolated to zero applied field a value of 0.84 eV is obtained. If this would only be due to an image potential barrier R_0 would amount to 1.42 Å which is very low considering the size of p-EFTP or even of a single triphenylamine moiety. This means that part of the barrier must be due to the primary injection step

$$E_a = \Delta U + \Delta H^o_{inj} \tag{11}$$

One can also try to find out the barrier, $\Delta H^o_{\mathrm{inj}}$ (Fig. 10) for the primary hole injection by combining experimental energy levels of p-EFTP in solution with data of anthracene in solution and in single crystals. In a solvent of medium polarity (CH_2Cl_2) the oxidation potential of p-EFTP[30] is 0.822 V versus the SCE while that of anthracene amounts to 1.34 V versus the SCE.[31] As anthracene and the active site (a triphenylamine moiety) in p-EFTP[30] have nearly the same size the dif-

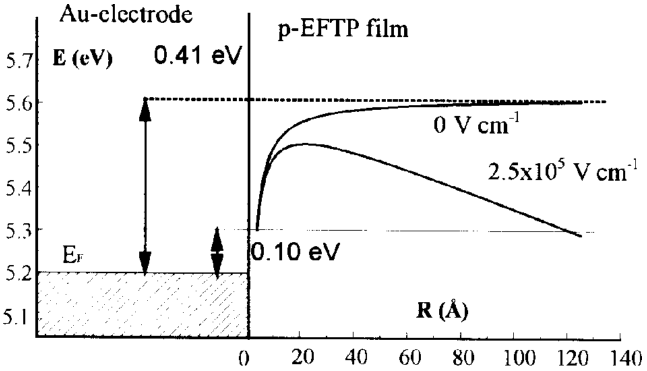

Figure 10. Energy levels at the interface between a gold electrode and a molecular dispersion of p-EFTP in polycarbonate.

ference of the ionization potentials will also be close to 0.53 eV. As the dielectric constant and polarizability of the polymer film approach those of perylene or anthracene single crystals, the polarization energy and image charge potential experienced by a molecule at the interface will be in a first approximation similar in both systems. Hence when the energy of the HOMO of an anthracene molecule in the ab-plane of single crystal interfacing water or a metal amounts 5.83 eV[2,21] one can estimate that energy of the HOMO of a p-EFTP molecule close to the interface equals 5.30 V. As the Fermi-level of gold is between 4.7[32,33] and 5.2 V below[34,35] the vacuum level, $\Delta H^{o}_{\mathrm{inj}}$ should be close to 0.10 eV (0.60 eV for a Fermi-level at 4.7 V). For R_0 equal to 4 Å, ΔU amounts to 0.30 eV, yielding a barrier (and E_a) of 0.40 eV (0.90 eV for E_F = 4.7 eV). This is smaller than the experimental value of E_a extrapolated to zero field when the most often used value of 5.2 V is used for the Fermi-level of gold. Here one should consider that depending upon the way the gold electrode was deposited[36] the hole current injected into a perylene single crystal could change by two orders of magnitude.[36] A possible reason for this discrepancy could be that the Fermi-level in this polycrystalline, evaporated electrode differs from that of a gold single crystal or an interaction between the transport molecules and the evaporated gold.[32,37] While gold evaporated on mica or glass substrata forms, especially when the substratum is heated,[38] a mosaic of predominantly (111) crystals, on organic films a cracked polycrystalline film still consisting for 2/3 of (111) phases is formed.[39–41] Even if 1/3 of the surface of the organic layer is covered by other phases with a larger work function those phases will contribute little to the current which will still mainly be carried by the (111) phases. Therefore this effect alone cannot explain the discrepancy between the estimated barrier and the observed activation energy.

It is unlikely that this discrepancy is linked to diagonal disorder in the transport material[8] as Monte Carlo simulations[9,10,42] suggest that the latter effect would decrease rather than increase the activation energy for charge injection. The latter simulations are confirmed by the fact the quantum yield of exciton dissociation in dispersions of hole[14,15,43] and electron[16] transport molecules in a polymer is nearly temperature independent.

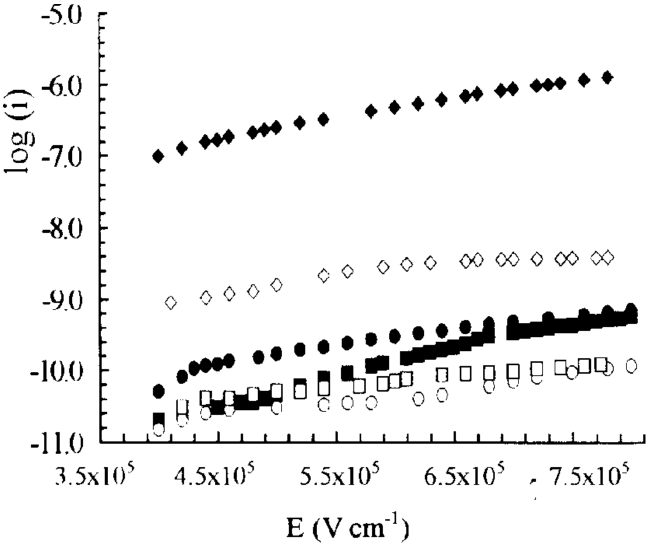

Figure 11. Influence of the applied field , electrode polarity and temperature upon the currents injected by a gallium electrode in a 40% molecular dispersion of ADCMI in polycarbonate; ■: gallium electrode negative, 309 K, ●: gallium electrode negative, 323 K, ◆: gallium electrode negative, 343 K, ❑: gallium electrode positive, 309 K, **O**: gallium electrode positive, 323 K, ◇: gallium electrode positive, 343 K.

Injection in ADCMI. For p-EFTP earlier experiments suggested, by taking into account the direction of the applied field and the chemical composition of the evaporated metal electrode that under all conditions the major part of the current density was carried by holes.[17] As for ADCMI transport by electrons was expected, a gallium drop was chosen as a top-electrode with a low work function (4.2 V).[44] As shown in Fig. 11 both at 310 K, 323 K and at 343 K the current density through a 10 μ thick layer of a 40% dispersion of ADCMI in polycarbonate was larger when the top electrode was negative, suggesting injection of electrons by the gallium electrode or of holes by the aluminum back electrode. Due to the large oxidation potential of ADCMI, it is highly unlikely that the latter process would yield a larger current density than the hole current injected by the same electrodes in a p-EFTP film.[17] The larger current density at 343 K is probably not only due to a more efficient injection but perhaps also to a better contact between the gallium electrode and the polymer film due to a decreased surface tension of the gallium drop at higher temperature. Increasing the ADCMI concentration to 50 and 60% increases the current density observed both with a positive and negative gallium top electrode (Fig. 12).

As the mobility of the electrons in the dispersion of ADCMI in polycarbonate is known from time-of-flight experiments,[16] the space charge limited current density,[45] j_{SCLC} (in $\mathrm{Acm^{-2}}$) can be calculated using Eq. 12 (Table I).

$$j_{SCLC} = \frac{9}{8}\mu 4\pi\varepsilon_0\varepsilon_r\frac{V^2}{\ell^3} \qquad (12)$$

In Eq. 12, V corresponds to the applied voltage and ℓ to the thickness of the sample. μ (in $\mathrm{cm^2\,s^{-1}V^{-1}}$) corresponds to the electron mobility determined for time-of-flight experiments[16] while ε_r is the dielectric constant of the sample for which a value of 3 is used. ε_o (8.85×10^{-14}

TABLE I. Space Charge Limitation of Electron Currents Injected by a Gallium Electrode in a Dispersion of a DCMI In Polycarbonate at 2.5 × 10⁵ V Cm⁻¹

T (K)	Concentration	$\mu(\vec{E} = 0)$ (cm²V⁻¹s⁻¹)	ℓ (cm)	j_{SCL} (Acm⁻²)	j_{exp} (Acm⁻²)
309	40%	4.1×10^{-9}	1.0×10^{-4}	3.8×10^{-5}	4.5×10^{-11}
	60%	7.6×10^{-8}	1.1×10^{-4}	6.5×10^{-5}	1.2×10^{-8}
323	40%	1.1×10^{-8}	1.0×10^{-4}	1.0×10^{-4}	1.7×10^{-10}
	60%	1.6×10^{-7}	1.1×10^{-4}	1.3×10^{-4}	2.8×10^{-6}
343	40%	3.8×10^{-8}	1.0×10^{-4}	3.6×10^{-4}	2.6×10^{-7}
	60%	3.9×10^{-7}	1.1×10^{-4}	3.3×10^{-4}	1.2×10^{-4}

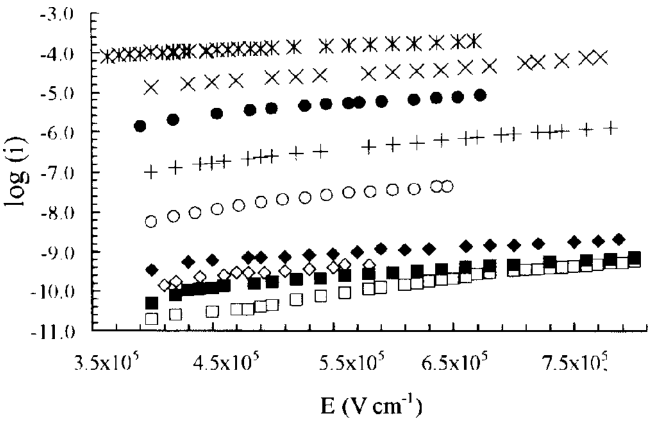

Figure 12. Influence of the applied field, temperature and concentration upon the currents injected by a gallium electrode in a molecular dispersion of ADCMI in polycarbonate; the gallium electrode is negative: ❑: 40%, 309 K, ■: 40% 323 K, +: 40%, 343 K, ◇: 50%, 309 K, ◆: 50%, 323 K, x: 50%, 343 K, **O**: 60%, 309 K, ●: 60%, 323 K, *: 60%, 343 K.

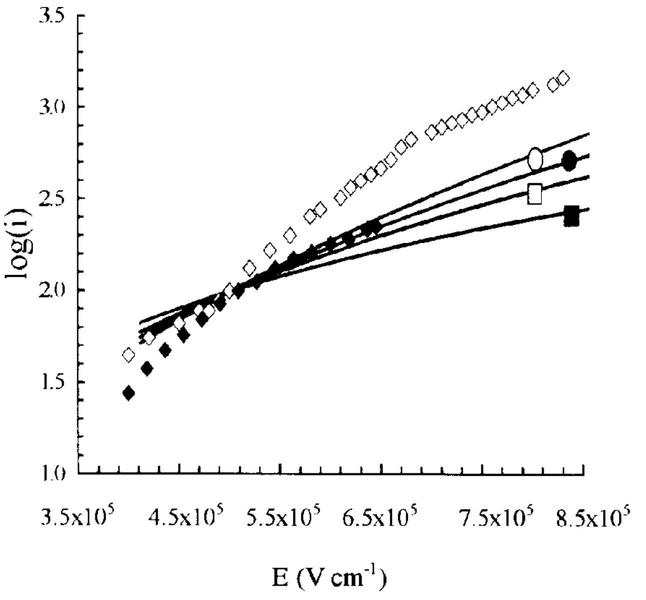

Figure 13. Field and concentration dependence of the injected electron current and field dependence the rate constant of escape of the electrons in the bulk for a dispersion of ADCMI in polycarbonate. The gallium electrode is negative; the currents and rate constants are normalized at 5.0 × 10⁵ V cm⁻¹; ◇: 40% ADCMI, ◆: 60% ADCMI, **O**: R_0 = 2 Å, λ: 4 R_0 = Å, ❑: R_0 = 6 Å, ■: R_0 = 10 Å.

CV⁻¹ cm⁻¹) is the permittivity of vacuum. While for the highest concentration of ADCMI and at 343 K the current density matches that of space charge limited current (SCLC) it is one or more orders of magnitude smaller at lower temperature or for a lower concentration of ADCMI. Considering the tendency of ADCMI to crystallize,[46,47] the large current densities found at 343 K or in the 60% samples are probably due to the formation of microcrystals. The latter effect can deteriorate the mechanical quality of the film and allow the formation of pinholes through which the gallium can diffuse.

At a concentration of 40% and at lower temperature the slope of the double logarithmic plot of the current density versus the applied field varies between 3.3 ± 0.1 and 5.20 ± 0.1 which again contradicts the occurrence of a SCLC characterized by a slope of two.

The activation energy of the current calculated over the temperature range between 310 K and 333 K amounts to 0.75 ± 0.1 eV and 0.95 ± 0.1 eV for the 40% and 50% samples respectively. Between 4.5 × 10⁵ V cm⁻¹ and 6.0 × 10⁵ V cm⁻¹ this activation energy is independent of the applied field. These data differ considerably from those obtained for p-EFTP where a clear decrease of the activation energy upon increasing the applied field was observed.[17] In the framework of the Willig-Gerischer model[2,21] the current density would be given by Eq. 5. Hence, for a suitable value of R_0, a logarithmic plot of the experimental values of the current density should be parallel to that of the calculated values of k_{esc}.

Figure 13 shows the field dependence of the current density and of k_{esc} for several values of R_0 and normalized at 5.0 × 10⁵ V cm⁻¹. Although the field dependence of current density parallels that of k_{esc} the agreement is not quantitative for any realistic value of R_0. As observed for hole injection into p-EFTP the current density increases faster than k_{esc}. This can could be attributed to disorder effects[8,9] or to the field dependence of v_{inj}.[2,21]

The Rate Constant for the Primary Injection Step. Based on Eq. 9 the rate constant for the pimary injection step k_{ox} (cm s⁻¹) can be obtained using following expression.

$$k_{ox} = \frac{jk_{rec}}{\mu kTN_{VB}} \frac{\int_{R_0}^{\infty} \exp\left[\frac{-U(R)}{kT}\right] dR}{\exp\left[\frac{-U(R_0)}{kT}\right]} \qquad (13)$$

Besides μ, which is known from time-of-flight experiments,[2,14-16,48] Eq. 13 contains three more parameters R_0, N_{VB} and k_{rec}. For anthracene and perylene single crys-

TABLE II. Influence of the Barrier on the Rate Constant for Charge Carrier Injection into Molecular Dispersions and Single Crystals

	40% ADCMI in PC[a]	50% pEFTP in PC[b]	50% pEFTP in PC[c]	anthracene[b]	perylene[b]	perylene[b]
ΔG° ($\vec{E} = 0$) (eV)	0.50[e]	0.10[d]	1.10[d]	0.63[d]	0.17[d]	0.17[d]
N_{VB} (cm^{-3})	8.135×10^{20}	9.230×10^{20}	9.230×10^{20}	4.33×10^{21}	3.20×10^{21}	3.20×10^{21}
μ($\vec{E} = 0$) ($cm^2V^{-1}s^{-1}$)	5.9×10^{-8}	9.7×10^{-6}	9.7×10^{-6}	8.5×10^{-1}	3.0×10^{-1}	3.0×10^{-1}
3.0×10^4 V cm^{-1}						
j (Acm^{-2})	—	1.8×10^{-10}	—	3.0×10^{-11}	1.0×10^{-8}	1.0×10^{-10}
k_{esc} (cms^{-1})	—	5.1×10^{-6}	—	4.4×10^{-1}	1.6×10^{-1}	1.6×10^{-1}
$k_{esc}/k_{esc}+k_{rec}$	—	5.1×10^{-11}	—	4.4×10^{-6}	1.6×10^{-6}	1.6×10^{-6}
k_{ox} (cms^{-1})	—	2.4×10^{-2}	—	9.7×10^{-9}	1.2×10^{-5}	1.2×10^{-7}
2.5×10^5 V cm^{-1}						
j (Acm^{-2})	1.1×10^{-11}	4.6×10^{-7}	1.73×10^{-11}	—	—	—
k_{esc} (cms^{-1})	2.7×10^{-6}	3.3×10^{-4}	3.3×10^{-4}	—	—	—
$k_{esc}/k_{esc}+k_{rec}$	2.7×10^{-11}	3.3×10^{-9}	3.3×10^{-9}	—	—	—
k_{ox} (cms^{-1})	3.0×10^{-3}	9.5×10^{-1}	3.6×10^{-5}	—	—	—

a) electron injection by a gallium electrode

b) hole injection by a gold electrode,

c) hole injection by an aluminum electrode, using 5.2 eV for the Fermi-energy[34,35] of gold,

d) using 4.1 eV for the electron affinity of a chloranil single crystal

tals[2,21-24] R_0 was close to 4 Å and a similar value can be assumed for p-EFTP or ADCMI as the ADCMI moiety or a single triphenyl amine moiety[29] have a size similar to anthracene. N_{VB} can be calculated from the sample preparation and amounts to 4.33×10^{21} cm^{-3}, 9.23×10^{20} cm^{-3} and 8.135×10^{20} cm^{-3} for an anthracene single crystal,[2,49] a 50% dispersion of p-EFTP in polycarbonate and a 40% dispersion of ADCMI in polycarbonate. For perylene single crystals N_{VB} amounts[2,50] to 3.2×10^{21} cm^{-3}. While k_{rec} has not been determined absolutely at a metal electrode, it should, taking into account the large density of energetically accessible states above the Fermi-level (below the Fermi-level in the case of hole injection) be put equal to the maximum possible rate for an electron transfer process[2,51-55] corresponding to 10^5 cm s^{-1}. In this way the values of k_{ox} given in Table II are obtained. Up to an applied field of 2.5×10^5 V cm^{-1} the ratio $k_{esc}/k_{esc}+k_{rec}$ was always below 3×10^{-4}. This means that even if k_{rec} would only amount to 3×10^3 cm s^{-1} it would still be much larger than k_{esc}. Hence both at 3×10^4 V cm^{-1} and 2.5×10^5 V cm^{-1} the current is controlled by the efficiency of the escape of the injected charge carriers from the image potential well. The currents as well as the values of k_{ox}, obtained for the molecular dispersions could be compared to those obtained for hole injection by a gold electrode into organic single crystals.[36] From the ionization potential of a molecule at the interface with a metal or water, which amounts to 5.83 and 5.37 eV for anthracene and perylene respectively[2,21] the free energy difference for the primary injection step could also be calculated for the latter systems. The electron affinity of ADCMI dispersed in polycarbonate amounts to 3.49 to 3.69 eV, taking into account the difference between the reduction potential of ADCMI[16,46] (–0.60 V versus SCE) and chloranil[56] (+0.01 V versus SCE) and the electron affinity of a chloranil single crystal[57-60] (4.10 to 4.30 eV). Due to the image potential at the metal interface the negative charge will have a further stabilization of 0.31 eV in ADCMI molecules at the interface, yielding a total energy of 3.80 to 4.00 V for the lowest unoccupied orbital at the interface. This yields a free energy difference ΔG° of 0.40 to 0.20 eV for the primary injection step. When one considers only data obtained for polymer dispersions or data obtained for single crystals, k_{ox} increases when the free energy difference ΔG° becomes smaller. However, when both types of samples are compared there is no clear trend. This should be attributed[9] to the presence of diagonal disorder[8,14] in the latter samples, which allows injection of electrons in the lower tail of the conduction band or of holes in the upper tail of the valence band. Furthermore the exact structure of the interface between the metal electrode and the organic insulator is also important as for the same combination of perylene and a gold electrode, values of k_{ox} differing by two orders of magnitude[36] are obtained. This difference was attributed to the way the gold electrodes were deposited.[36]

Conclusions

The present results show that for a range of electrodes, charge transport molecules and matrices, injection of charge carriers into molecular dispersions can be described as a an electron or hole transfer from the metal to a transport molecule in contact with the metal, followed by competition between recombination and escape to the bulk of the transport layer. The scaling of the current density with the charge carrier mobility, in samples where the current densities vary more than one order of magnitude, is due to the proportionality between the rate constant of the escape process and the current density. Also the general features of plots of the current densities versus the applied field more resemble[17,18] those developed for charge carrier injection into organic single crystals than those developed for electron-emission in vacuum or semiconductors. Furthermore[17] while application of e.g., the Fowler Nordheim model[1] yielded for the limiting current values that were thirteen orders of magnitude too small compared to those obtained for charge carrier injection in vacuum or in Si,[29] application of the Willig-Gerischer model yielded for the rate constant for the primary injection step values that were, considering the free energy change, only two or three orders of magnitude larger than those obtained for organic single crystals. Here one has to take into account that for the same combination of electrode (gold) and insulator (perylene) values of k_{ox} differing by more than one order of magnitude were obtained.[36] This discrepancy can furthermore be explained[9] considering the presence of diagonal disorder[8] in the present samples. While already for single crystals[36] the escape of the injected charge carrier was much slower than recombination this will be *a fortiori* the case for the present samples characterized by a lower[13,16] charge carrier mobility.

In spite of the agreement with results obtained for single crystals there remain several discrepancies:

1. The current densities show more important field dependence than allowed by Eq. 2 for any reasonable value of R_0. The deviations form the features predicted for R_0 = 4 Å, are the same for different electrodes, matrices and types of charge carriers. Furthermore a similar discrepancy is observed for photosensitized hole injection in a molecular dispersion of p-EFTP, where the first hole injection step is clearly exothermic.[18] This suggests that the deviations are not related to the first charge injection step but to the field dependence of the subsequent escape process described by k_{esc}. This process has clearly more important field dependence than predicted by Eq. 2. Although it is tempting to attribute this process to the field dependence of the hole or electron mobility,[8,13–16] one should realize that in the image potential well, the actual field opposes the applied field. It is for the moment unclear if the discrepancy can attributed to disorder effects.[9] Furthermore one can conclude that the first electron transfer step probably does not occur over a distance exceeding 10 Å. In the latter case the field dependence of the current density would also depend upon the free energy change of this primary charge transfer step.
2. A further problem is situated in the field dependence of the activation energy for hole injection by a gold electrode in 50% dispersion of p-EFTP in polycarbonate. This is much larger than predicted by Eq. 10. This could be due to disorder effects.[9]
3. The activation energy for hole injection by a gold electrode in 50% dispersion of p-EFTP in polycarbonate, extrapolated to zero field, is 0.4 eV larger than expected on basis of the most commonly used value for the work function of gold and the oxidation potential of p-EFTP. This is probably not due to the occurrence of diagonal disorder as the latter effect was predicted to decrease[9] this activation energy. Those predictions were verified for intrinsic photogeneration of charge carriers in molecular dispersions of pEFTP[13–15,43] and ADCMI.[16] It can perhaps be due to a different Fermi-level in the polycrystalline vapor deposited gold compared to the monocrystalline gold for which the Fermi-level[32] was determined. For the ADCMI samples the small temperature range where the samples could be studied in a reliable way (309 K to 323 K) makes an accurate determination of activation properties and their field dependence more difficult.

Although the model developed for single crystals gives a good qualitative description of the hole or electron injection in disordered organic solids, it is clear that quantitative agreement requires at least the inclusion of diagonal and non-diagonal disorder. The latter will however nearly completely exclude an analytical description of this process. Furthermore some observations on the present samples do not agree with the trends imposed by the disorder model. While it is suggested that diagonal disorder decreases the activation energy compared to the difference between the ionization potential or electron affinity of the transport material and the Fermi-energy of the metal, the opposite effect is observed for a 50% dispersion of p-EFTP in polycarbonate. For the dispersion of ADCMI in polycarbonate the situation is less clear due to the uncertainty on the electron affinity of the chloranil crystal, used to scale the reduction potentials of the electron acceptors and their electron affinities.

One of the basic differences of injection into a disordered molecular material compared to an inorganic semiconductor is the relatively small thermalization length of the injected charge carriers. In this way they resemble liquids[61,62] or organic molecular crystals.[22,63] Apparently this contradicts the observations for intramolecular[64-67] electron or hole transfer, for electron or hole transfer in Langmuir-Blodgett-films[68–73] and for electrochemical electron transfer at electrodes covered by self adsorbed or deposited monolayers.[74–80] While a long distance electron transfer is only observed through conjugated chains[67,79,80] or through all-trans saturated spacers[64-72,77] the rate of intermolecular electron transfer in disordered glasses decreases by a factor of ten when the distance increases by 1 Å[81,82] in disordered glasses. As the latter resemble the dispersions of organic molecules in a polymer matrix it is not surprising that no strong evidence for a long distance injection is observed. The rate for the primary electron transfer step is expected to decrease by a factor of three (all-trans saturated spacers) to ten (disordered THF glass) when the distance increases by one Å. Hence the rate constant for the escape process should at least increase to the same extent when the injected hole is thermalized one Å farther away from the interface. This would correspond to a decrease of the image potential by 0.03 to 0.06 eV, which is impossible at distances larger than 5 to 6 Å away from the interface.

Acknowledgements. M. Van der Auweraer is a "Onderzoeksdirecteur" of the Fonds voor Wetenschappelijk Onderzoek (F. W. O.). J. Rommens thanks the "Vlaams instituut voor de bevordering van het wetenschappelijk en technologisch onderzoek in de industrie (I. W. T.)" for financial support. The continuing support of the "Fonds voor Wetenschappelijk Onderzoek", the "Nationale Loterij" and the DWTC through IUAP IV-11 is gratefully acknowledged. The authors thank D. Terrell (Agfa-Gevaert) for providing p-EFTP films and ADCMI-films.

References

1. S. M. Sze, *Physics of Semiconductor Devices*, John Wiley & Sons, New York, 1981, pp. 245–312.
2. F. Willig, *Advances in Electrochemistry and Electrochemical Engineering*, Vol. 12, C. W. Tobias and G. Gerischer, Eds., Wiley, New York, 1981, pp. 1–111.
3. M. A. Abkowitz, H. Antoniadis, J. S. Facci, B. R. Hsieh and M. Stolka, *Synth. Metals* **67,** 187 (1994).
4. M. Abkowitz, J. S. Facci and M. Stolka, *Chem. Phys.* **177,** 783 (1993).
5. H. Antoniadis, M. Abkowitz, B. R. Hsieh, S. A. Jenekhe, and M. Stolka, *Mat. Res. Soc. Symp. Proc.* **328,** 377 (1994).
6. P. M. Borsenberger and D. S. Weiss, *Organic Photoreceptors for Imaging Systems*, M. Dekker Inc, New York, 1993.
7. P. E. Burrows, S. R. Forrest and M. E. Thompson, *Current Opinion in Solid State & Materials Science* **2,** 236 (1997).
8. H. Bässler, *Phys. Stat. Sol. (b)* **175,** 15 (1993).
9. V. I. Arkhipov, E. V. Emelianova, Y. H. Tak, and H. Bässler, *J. Appl. Phys.* **84,** 848 (1998).
10. U. Albrecht and H. Bässler, *Chem. Phys. Lett.* **235,** 389 (1995).
11. S. Barth, D. Hertel, Y. H. Tak, H. Bässler, and H. H. Hörhold, *Chem. Phys. Lett.* **274,** 165 (1997).
12. S. Barth, M. Deussen and H. Bässler, *Phil. Trans. Roy. Soc. London A* **355,** 749 (1997).
13. M. Van der Auweraer, F. C. De Schryver, P. M. Borsenberger, and H. Bässler, *Adv. Mater.* **6,** 199 (1994).
14. M. Van der Auweraer, G. Verbeek, F. C. De Schryver, and P. M. Borsenberger, *Chem. Phys.* **190,** 31 (1995).
15. B. Hartenstein, H. Bässler, S. Heun, P. Borsenberger, M. Van der Auweraer, and F.C. De Schryver, *Chem. Phys.* **191,** 321 (1995).
16. J. Rommens, M. Van der Auweraer, F. C. De Schryver, D. Terrell and S. De Meutter, *J. Phys. Chem.* **100,** 10673 (1996).

17. J. Rommens, M. Van der Auweraer and F. C. De Schryver, *J. Phys. Chem.* **101,** 3081 (1997).
18. J. Rommens, M. Van der Auweraer and F. C. De Schryver, *Chem. Phys. Lett.* **294,** 334 (1998).
19. M. Van der Auweraer, F. C. De Schryver, G. Verbeek, C. Geelen, D. Terrell, and S. De Meutter, European Patent 0-349-034-B1 (January 12, 1994) Application 89201552.0 (June 15, 89).
20. D. R. Terrell, F. C. De Schryver, C. Geelen, M. Monbaliu, S. De Meutter, M. Van der Auweraer, and G. M. Verbeek, European Patent 0 537-808-B1 (Nov. 6, 1996) Application 922002585.3 (Aug. 25, 1992).
21. H. Gerischer and F. Willig, *Topics in Current Chemistry* **61,** 31 (1976).
22. K.-P. Charlé and F. Willig, *Chem. Phys. Lett.* **57,** 253 (1978).
23. N. Müller, G. Papier, K.-P. Charlé, and F. Willig, *Ber. Buns. Phys. Chem.* **83,** 131 (1979).
24. F. Willig, *Chem. Phys. Lett.* **40,** 331 (1976).
25. E. A. Silinsh and V. Cápek, *Organic Molecular Crystals*, AIP press, American Institute of Physics, New York, 1994.
26. A. J. Heeger, I. D. Parker and Y. Yang, *Synth. Metals* **67,** 23 (1994).
27. H. Vestweber, J. Pommerehne, R. Sander, R. F. Mahrt, A. Greiner, W. Heitz, and H. Bässler, *Synth. Metals* **68,** 263 (1995).
28. J. J. O'Dwyer, *The Theory of Electrical Conduction and Breakdown in Solid Dielectrics*, Clarendon Press, Oxford, 1973.
29. J. M. Andrews, *Solid State Electronics* **13,** 11 (1970).
30. J. Bonvoisin, J-P. Launay, M. Van der Auweraer and F. C. De Schryver, *J. Phys. Chem.* **98,** 5052 (1994).
31. A. Bard, *Discussions Faraday Society* **45,** 167 (1968).
32. E. E. Huber, *Appl. Physics Letters* **8,** 169 (1969).
33. P. C. Rieke and N. R. Armstrong, *J. Am. Chem. Soc.* **106,** 47 (1984).
34. D. E. Eastman, *Phys. Rev. B* **2,** 1 (1970).
35. C. Rivière, *Work Function Measurements and Results*, Metallurgy Div. at Energy Res. Establ, Harwell, Berkshire, UK, 1971.
36. B. Korsch, F. Willig, H. J. Gaehrs, and B. Tesche, *Phys. Stat. Sol. (a)* **33,** 461 (1976).
37. A. Ioannidis, J. Facci and M. Abkowitz, *Proc. ECME97*, Cambridge 1997, p. 70.
38. M. Hegner, P. Wagner and G. Semnza, *Surf. Sci.* **291,** 39 (1993).
39. A. Ioannidis, J. S. Facci and M. A. Abkowitz, *J. Appl. Phys.* **84,** 1439 (1998).
40. C. C. Chidsey, D. N. Loiacono, T. Sleator, and S. Nakahara, *Surface Sci.* **200,** 45 (1988).
41. T. P. Nguyen and S. de Vos, *Vacuum* **47,** 1153 (1996).
42. K. Watanabe, T. Asahi and H. Masuhara, *J. Phys. Chem.* **100,** 18346 (1996).
43. G. Verbeek, Ph.D. Thesis Katholieke Universiteit Leuven, Leuven, Belgium. 1992.
44. *Handbook of Chemistry and Physics,* D. R. Lide, Ed., CRC Press, Boca Raton, 73rd ed., 1992–1993, Chap. 12, p. 108 (1992–1993).
45. A. Rose, *Phys. Rev.* **97,** 1538 (1955).
46. P. M. Borsenberger, E. H. Magin, M. Van der Auweraer, and F. C. De Schryver, *Phys. Stat. Sol. (b)* **186,** 217 (1994).
47. J. Rommens, M. Van der Auweraer, F. C. De Schryver and P. M. Borsenberger, *Adv. Mat.* **7,** 574 (1995).
48. N. Karl, *Organic Semiconductors* in Landolt-Bornstein, Group III, Vol. 17, Semiconductors, Springer-Verlag Berlin, p. 135.
49. E. A. Silinsh, *Organic Molecular Crystals*, Springer Series in Solid-State Sciences, M. Cardona and H.-J. Queisser, Eds., Springer-Verlag, Berlin, 1989, p. 14.
50. E. A. Silinsh, *Organic Molecular Crystals*, Springer Series in Solid-State Sciences, M. Cardona and H.-J. Queisser, Eds., Springer-Verlag, Berlin, 1989, p. 23.
51. R. A. Marcus, *Ann. Rev. Phys. Chem.* **13,** 155 (1964).
52. N. R. Kestner and J. Logan and J. Jortner, *J. Phys. Chem.* **78,** 2148 (1974).
53. J. Jortner, *J. Chem. Phys.* **64,** 4680 (1976).
54. R. A. Marcus, J. Chem. Phys. **81,** 4494 (1984).
55. H. Sumi and R. A. Marcus, *J. Chem. Phys.* **84,** 4894 (1986).
56. M. E. Peover, *J. Chem. Soc.* 4540 (1962).
57. H. Killesreiter, *Ber Bunsenges. Phys. Chem.* **77,** 938 (1973).
58. M.-E. Michel-Beyerle and F. Willig, *Solid State Commun.* **7,** 913 (1969).
59. M.-E. Michel-Beyerle and R. E. Haberkorn, *Z. Naturf.* **27a,** 1496 (1972).
60. R. Haberkorn, W. Harengel, H.-P. Braun and M.-E. Michel-Beyerle, *Ber. Bunsenges. Phys. Chem.* **77,** 928 (1973).
61. B. Holroyd, B. K. Dietrich and H. A. Schwarz, *J. Phys. Chem.* **76,** 3794 (1972).
62. P. Smejtek, M. Silver and K. S. Dy, *J. Chem. Phys.* **59,** 1374 (1973).
63. R. R.Chance and C. L. Braun, *J. Chem. Phys.* **64,** 3573 (1976).
64. J. R.Miller, J. V. Beitz and R. K. Huddleston, *J. Am. Chem. Soc.* **106,** 5057 (1984).
65. L. T. Calcaterra, G. L. Closs and J. R. Miller, *J. Am. Chem. Soc.* **105,** 670 (1983).
66. J. M. Warman, M. P. de Haas, M. N. Paddon-Row, H. Cotsaris, N. S. Hush, H. Oevering, and J. W. Verhoeven, *Nature* **320,** 615 (1986).
67. P. Finckh, H. Heitele, M. Volk and M. E. Michel-Beyerle, *J. Phys. Chem.* **92,** 6584 (1988).
68. K. P. Seefeld, D. Möbius and H. Kuhn, *Helv. Chim. Acta* **60,** 2608 (1977).
69. D. Möbius, *Ber. Bunsenges. Phys. Chem.* **82,** 848 (1978).
70. H. Kuhn, *Light-Induced Charge Separation in Biology and Chemistry*, H. Gerischer and J. J. Katz, Eds., Dahlem Konferenzen Berlin, 1979, p. 151.
71. H. Kuhn, *Modern Trends of Colloid Science in Chemistry and Biology*, Birkhauser Verlag, Basel, 1985, p. 97.
72. M. Van der Auweraer, G. Biesmans, B. Verschuere, F. C. De Schryver, and F. Willig, *Langmuir* **3,** 992 (1987).
73. A. Itaya, M. Van der Auweraer, B. Verschuere, and F. C. De Schryver, *Israel J. Chem.* **31,** 169 (1991).
74. M. A. Abkowitz, H. A. Mizes and J. S. Facci, *Appl. Phys. Lett.* **66,** 1288 (1995).
75. M. D. Lin, Ch. R. Leidner and J. S. Facci, *J. Phys. Chem.* **96,** 2804 (1992).
76. X. Liang-Hong Guo, J. S. Facci and G. Mc Lendon, *J. Phys. Chem.* **99,** 8458 (1995).
77. J. F. Smalley, S. W. Feldberg, C. E. D. Chidsey, M. R. Linford, M. D. Newton, and Y.-P. Liu, *J. Phys. Chem.* **99,** 13141 (1995).
78. A. J. Bard, H. D. Abruna, C. E. Chidsey, L. R. Faulkner, S. W. Feldberg, K. Itaya, M. Majda, O. Melroy, R. W. Murray, M. D. Porter, M. P. Soriaga, and H. S. White, *J. Phys. Chem.* **97,** 7147 (1993).
79. S. Creager, C. J. Yu, C. Bamdad, S. O'Connor, T. MacLean, E. Lam, Y. Chong, G. T. Olsen, J. Luo, M. Gozin, and J. F. Kayem, *J. Am. Chem. Soc.* **121,** 1059 (1999).
80. S. B. Sachs, S. P. Dudek, R. P. Hsung, L. R. Sita, J. F. Smalley, M. D. Newton, C. E. Chidsey, and S. W. Feldberg, *J. Am. Chem. Soc.* **119,** 10563 (1997).
81. J. R. Miller and J. V. Beitz, *J. Chem. Phys.* **74,** 6746 (1981).
82. J. R. Miller, J. A. Peeples, M. J. Schmitt and G. L.. Closs, *J. Am. Chem. Soc.* **104,** 6448 (1992).